GEOPHYSICAL RESEARCH LETTERS, VOL. 7, NO. 5, PAGES 293-296, MAY 1980

OBSERVATIONS OF A FREE-ENERGY SOURCE FOR INTENSE ELECTROSTATIC WAVES

W. S. Kurth, L. A. Frank, M. Ashour-Abdalla*, D. A. Gurnett, and B. G. Burek

Department of Physics and Astronomy, The University of Iowa, Iowa City, IA 52242

*Department of Physics and Institute of Geophysics and Planetary Physics, University of California, Los Angeles, CA 90024

Abstract. Significant progress has been made in understanding intense electrostatic waves near the upper hybrid resonance frequency in terms of the theory of multiharmonic cyclotron emissions using a classical loss-cone distribution function as a model. Recent observations by Hawkeye 1 and GEOS 1 have verified the existence of loss-cone distributions in association with the intense electrostatic wave events, however, other observations by Hawkeye and ISEE have indicated that loss cones are not always observable during the wave events, and in fact other forms of free energy may also be responsible for the instability. Now, for the first time, a positively sloped feature in the perpendicular distribution function has been uniquely identified with intense electrostatic wave activity. Correspondingly, we suggest that the theory is flexible under substantial modifications of the model distribution function.

Introduction

The study of electron cyclotron emissions has expanded rapidly within the past year in two significant areas. First, intense emissions at or near the upper hybrid resonance frequency have been explained in terms of a nonconvective instability in the cyclotron harmonic band encompassing the (cold) upper hybrid resonance frequency [Kurth et al., 1979a, b]. The upper hybrid resonance frequency, f_{UHR}, is $\sqrt{(f_p^-)^2 + (f_g^-)^2}$ where f_p^- is the electron plasma frequency and f_g^- is the electron gyrofrequency. The cold f_{UHR} is thought to be approximately equal to the total f_{UHR} during intense upper hybrid wave events because the ratio of the cold-to-hot electron density, n_c/n_h, is expected to be large from theoretical considerations [Ashour-Abdalla and Kennel, 1978a; Hubbard and Birmingham, 1978].

The second significant advance in the study of electron cyclotron emissions has come in the form of direct comparisons of simultaneous observations of the wave emissions and associated distribution functions with predictions of the theory [Rönnmark et al., 1978; Kurth et al., 1979b]. These comparisons are still in a necessarily qualitative state since the theory is linear while the waves almost certainly saturate nonlinearly. These comparisons indicate the theory correctly predicts the frequency, bandwidth, and polarization of intense upper hybrid resonance waves. The observations of the energetic electron distribution functions associated with the waves have been heretofore less than well understood, however. Lacking observational input, the theory is largely based on a loss-cone distribution similar to the form of Ashour-Abdalla and Kennel [1978b]. This form of the distribution function has been observed during intense upper hybrid events. [Rönnmark et al., 1978; Kurth et al., 1979a], but a one-to-one correspondence has not been demonstrated. In fact, Kurth et al. [1979a,b] show that other forms of free energy are present during some events, such as anisotropies and positive slopes with respect to the perpendicular velocity $v_\perp$. Again, a one-to-one correspondence has not been demonstrated for any event.

Now, for the first time, observations are available which provide convincing evidence for a source of free energy in the energetic electron distribution function which can be uniquely associated with intense electrostatic waves. This letter describes the observations of the free-energy source and discusses the implications of this development to the theory of electron cyclotron emissions.

Observations

The intense electrostatic waves of interest here have been described in detail by Kurth et al. [1979a]. Briefly, these emissions near f_{UHR} coincide with $(n + \frac{1}{2})f_g^-$ bands. The amplitudes of the waves range from ~ 1 to 20 mV m^{-1} and the electric field vectors of the waves are aligned nearly perpendicular to the geomagnetic field. Figure 1 shows a particularly striking example of these emissions. Illustrated are wave amplitudes as a function of time (abscissa) and frequency (ordinate). The darkest areas represent the most intense waves. The data are obtained from the University of Iowa plasma wave experiment onboard ISEE 1 [Gurnett et al., 1978]. The very intense wave turbulence at about 18 kHz between 1140 and 1146 UT is an example of the upper hybrid waves under consideration. The peak electric field during this time is 1.04 mV m^{-1} corresponding to an energy density of 4.4×10^{-17} erg $(cm)^{-3}$. The dark rectangular region at this time is the result of receiver distortion effects due to the large amplitudes of the waves. (Observations from IMP 6 and Hawkeye indicate there is no significant broadening of the emissions during the peak of the events [Kurth et al., 1979a].) The band of emission appears to be an intensification of a band which extends from as early as 1050 UT at 300 kHz to beyond 1230 UT near 6 kHz. Prior to 1140, the band is near the upper hybrid resonance frequency with a typical amplitude of a few μVm^{-1} and shows an abrupt decrease in frequency as the spacecraft exits the plasmasphere at 1109 UT. Beyond 1140, however, the band lies between the first two harmonics of the electron gyrofrequency, hence, is referred to as the $3f_g^-/2$ band. The intense waves occur, then, when $f_{UHR} \approx 3f_g^-/2$. This event illustrates well the tendency for these electrostatic waves to intensify when $f_{UHR} \approx (n + \frac{1}{2})f_g^-$. Also apparent in Figure 1 is a weak emission near $5f_g^-/2$ between about 1230 and 1310 UT and nonthermal continuum radiation after 1130 UT between about 10 kHz and 50 kHz.

Other changes in the wave spectrum during the time of the intense waves near f_{UHR} include a slight decrease in the amplitude of whistler mode waves just below f_g^- near 5 kHz and an enhancement of emissions below about 300 Hz. The spectral density of these low frequency waves is about 5×10^{-12} $V^2m^{-2}Hz^{-1}$ compared to about 5×10^{-10} $V^2m^{-2}Hz^{-1}$ for the band at f_{UHR}. Christiansen et al. [1978] have reported correlations between intense electrostatic waves near f_{UHR} and enhancements in the ELF frequency range.

A quadrispherical Lepedea [Frank et al., 1978] provides three dimensional plasma analysis simultaneously with the observations of the plasma wave receiver on ISEE. During the outbound pass of December 9, 1977, the analyzer was configured to measure electrons with energies between 221 eV and 45.6 keV at a rate which provides a complete, three dimensional analysis every eight minutes.

Figure 2 shows perspective plots of the electron distribution function, $f(v_\perp, v_\parallel)$, obtained before, during, and after the intense wave event illustrated in Figure 1. The two distributions in the upper portion of Figure 2 were taken immediately prior to the intense wave event. The distribution function in the lower left was obtained simultaneously with the detection of the in-

Paper number 80L0255.
0094-8276/80/0080L-0255$01.00

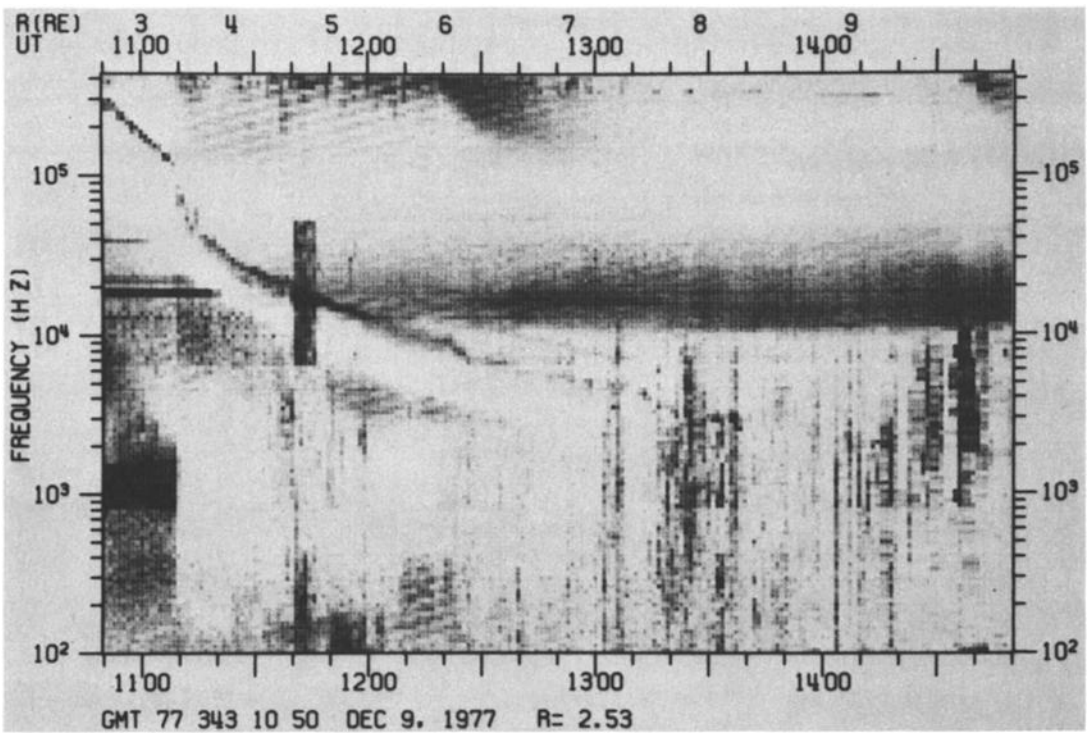

Fig. 1. An example of intense electrostatic waves at $(n + \frac{1}{2})f_e^-$ and f_{UHR}. The event lies between about 1140 and 1145 UT at about 18 kHz. At this time ISEE 1 is at 3.8 hours magnetic local time and at 38.1° magnetic latitude. The dark rectangular region surrounding the event is due to receiver distortion.

tense electrostatic waves. The lower right-hand plot shows the distribution gained just after the wave event.

All four distributions shown in Figure 2 have similar gross characteristics; a relatively isotropic two-temperature bi-Maxwellian form with densities and temperatures which are approximately the same in each. Each distribution has a weak beam-like feature parallel to $\vec{B}$ near 8 x 10^9 cm(sec)$^{-1}$. All show local irregularities in the warmer portions of the distribution which are most likely the result of poor counting statistics. The distribution obtained simultaneously with the intense electrostatic wave event, however, shows a well-organized relative maximum near 7.2 x 10^9 cm(sec)$^{-1}$ which extends to nearly the full range of pitch angles but, most importantly, at pitch angles near 90°. This relative maximum at large pitch angles necessarily implies a positive slope with respect to $v_\perp$ at slightly lower velocities. This feature does not appear at all in the velocity distributions from 1119 and 1145 UT and only very weakly at 1128 UT. While the relative maximum near 7.2 x 10^9 cm(sec)$^{-1}$ is not noticeably more intense than the statistical irregularities noted above, it is important that the feature is organized and extends in an orderly fashion over a range of phase space. This particular feature is observed by a number of different detectors and it is highly unlikely that statistical fluctuations could account for such an extended relative maximum.

Since a positive slope in the perpendicular velocity distribution provides a free-energy source to generate the electrostatic waves, it is useful to examine a cut of the distributions of Figure 2 at a pitch angle of 90°. These perpendicular velocity distributions are shown in Figure 3 using contours derived from averages over several detectors. The error bar represents the typical error in each of the curves. In this illustration it is obvious that a source of free energy exists during the interval 1136 to 1145 UT which does not exist immediately before or after. This is almost exactly the interval of greatest wave intensity as seen in Figure 1. In fact, the energies corresponding to ~ 7 x 10^9 cm(sec)$^{-1}$ were sampled between 1143 and 1144 UT. Hence, this almost certainly ties the positive slope free-energy source to the intense electrostatic emissions. The free energy density of the feature near 7.2 x 10^9 cm(sec)$^{-1}$ in Figure 2c is approximately 7 x 10^{-13} erg (cm)$^{-3}$ or more than a factor of 10^4 greater than the energy density in the waves. It is most probable that this positively sloped feature is the driver of the wave instability and not a causal effect of the waves, since it is unlikely that wave turbulence would create such an unstable distribution. The question of nonlinear effects of the waves on the electrons is treated further in the next section.

Figures 2 and 3 allow us to show the evolution of the 3-dimensional distribution function as the spacecraft moves from one plasma regime to the next. Earlier studies, such as those by Kurth et al. [1979a], were confined by viewing angle constraints which changed rapidly, hence, changes in the observations from one time period to the next could be just as easily attributed to a change in viewing geometry as to true changes in the distribution function. The ISEE instrumentation can easily show the existence of peculiar particle distribution functions which are highly localized in space or time.

Discussion

In the previous section we have shown simultaneous wave and plasma measurements which, for the first time, provide a cogent demonstration of a particular feature of the energetic electron distribution function acting as a driver of electrostatic cyclotron harmonic waves. The feature, in this case, is a local maximum in the electron velocity distribution at about 7.2 x 10^9 cm(sec)$^{-1}$ at virtually all pitch angles, that is, a spherical shell of hot electrons. A slice at 90° pitch angles, as shown in Figure 3, shows a ring or bump-on-tail-like feature with a definite positive slope which is a source of free energy. To within the temporal resolution of the quadrispherical Lepedea, the free-energy source appears concurrently with intense electrostatic turbulence near $3f_e^-/2$ and f_{UHR}.

We do not wish to imply that the distribution in Figures 2 and 3 is the only form which will drive electron cyclotron har-

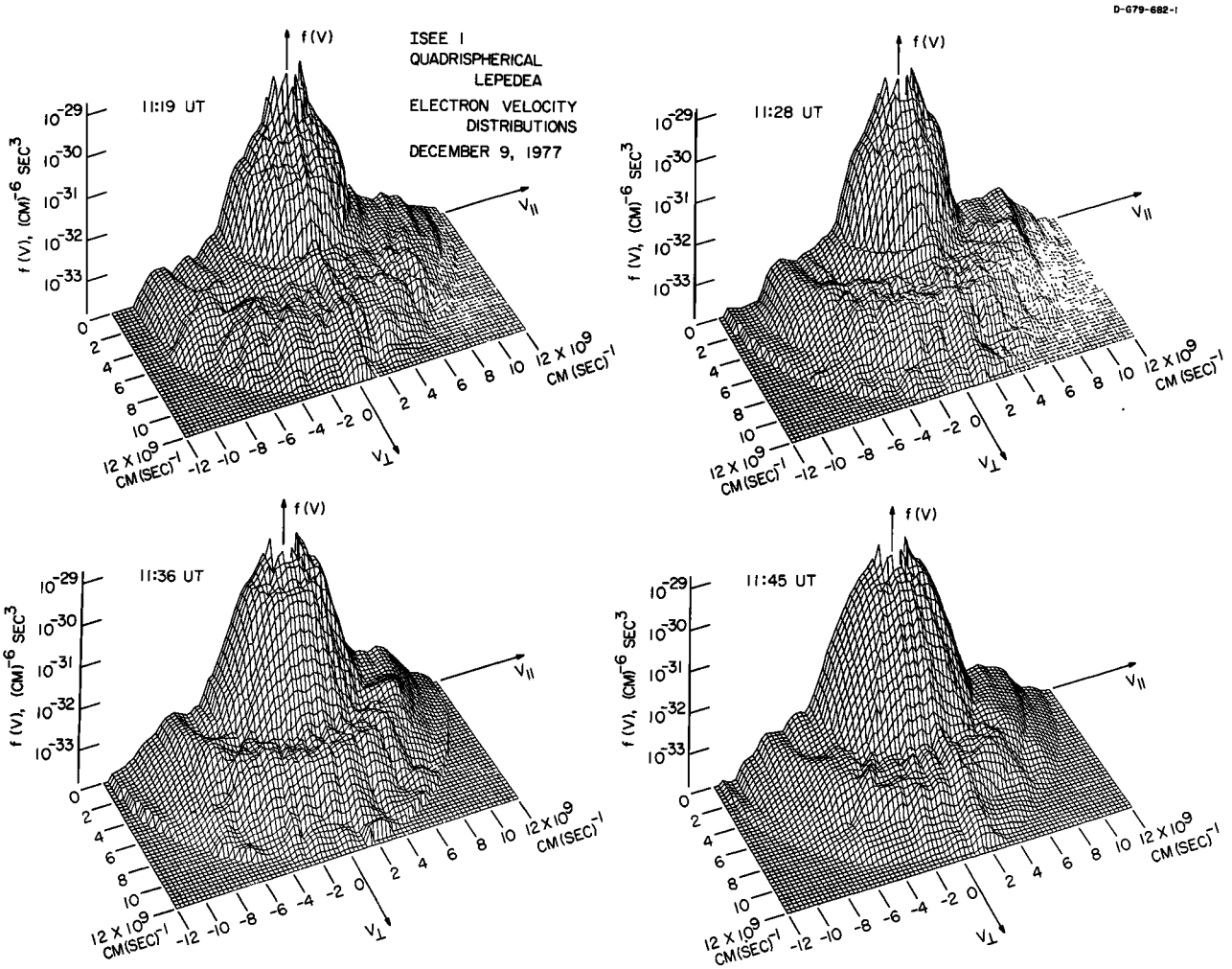

Fig. 2. A series of distribution functions obtained before, during and after the intense electrostatic wave event shown in Figure 1. Notice all have the same general form, except the distribution from 1136 UT shows a local maximum in the hot electron population at nearly all pitch angles near 7.2×10^9 cm(sec)$^{-1}$.

monic waves. On the contrary, we use the above observations to broaden our view of the odd half-harmonic emissions. Due to a lack of observational input until recently, the theory has utilized a loss-cone distribution similar to those assumed by Ashour-Abdalla and Kennel [1978b] and Hubbard and Birmingham [1978]. Observations by Rönnmark et al. [1978] and Kurth et al. [1979a] have confirmed the existence of loss-cone distributions concurrent with electrostatic waves (even though a one-to-one correspondence was not demonstrated). Kurth et al. [1979a,b] and Sentman et al. [1979], however, have shown evidence indicating other forms of the distribution may be important. The observations presented here confirm that other forms do, indeed, drive the electrostatic instabilities in some cases. Hence, it appears that a wide variety of forms may drive these waves. Certainly, the theory must be compatible with a variable model distribution.

The theory actually shows great flexibility to changes of the model distribution within the framework of the loss-cone formulation [Ashour-Abdalla and Kennel, 1978b]. Therefore, we expect the distribution in Figure 2 will also result in large spatial growth rates and/or non-convective instabilities. In several respects, the distribution in Figure 2 resembles the loss cone. Most important, both distributions show a positive slope with respect to $v_\perp$. Work is currently underway using a new analytic model of the perpendicular distribution function consisting of a cold core and a perpendicular beam which is similar to the distribution for 1136 UT in Figure 3. Initial results using $v_B = 2v_{th}$ where v_B is the beam velocity and v_{th} is the thermal spread of the beam gives large spatial growth rates and sometimes a non-convective instability in the first harmonic band. The theoretical investigation of the waves based on the perpendicular beam model indicates waves will be generated with features qualitatively similar to those using the loss-cone model. For example, the polarization is nearly the same using either model as is the bandwidth for positive growth.

Two questions are raised by the existence of an apparently unstable distribution accompanied by intense electrostatic waves. First, how was the distribution at 1136 UT in Figure 2 formed? Second, where are the nonlinear effects expected from the presence of the intense electrostatic waves? Unfortunately, these two questions are not entirely independent and the complete answer to one must also address the other. However, a relatively simple answer to the first question is suggested here. Suppose a population of hot electrons is injected from the plasma sheet near 90° pitch angle forming a highly anisotropic distribution near the equator with a relative maximum near 7.2×10^9 cm(sec)$^{-1}$. This distribution could then excite intense electrostatic waves which would, in turn, result in pitch angle scattering of the hot electrons. Hence, the feature at large pitch angles could diffuse into a hot shell similar to that shown in Figure 2.

We further suggest that the nonlinear effects which would be expected from the existence of the intense electrostatic waves

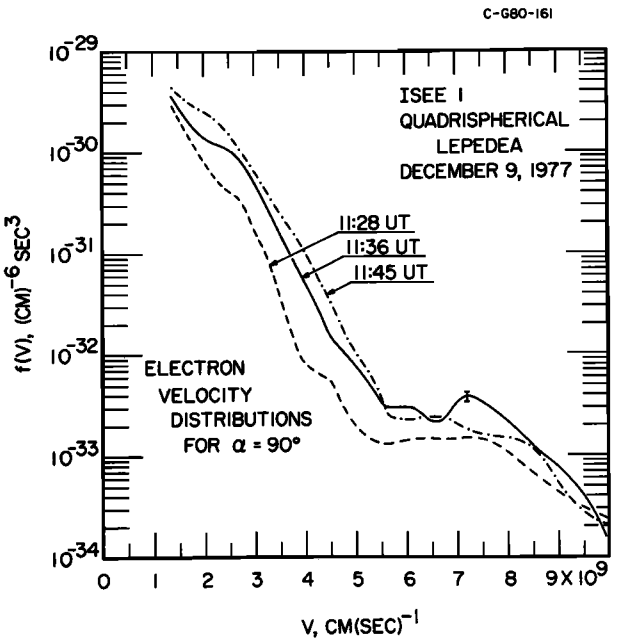

Fig. 3. Electron velocity distributions at pitch angle $\alpha = 90°$ for three of the perspective plots shown in Figure 3. Notice the distribution obtained during the interval 1136-1145 UT exhibits an obvious positive-sloped feature which does not appear in the distributions taken before or after the intense electrostatic wave event.

may be taking place primarily in the cold electron distribution at energies below the 221-eV threshold of the present Lepedea configuration. This suggestion is prompted by theoretical work which predicts much shorter time scales for the evolution (heating) of the cold electrons than for the hot electrons, if the ratio of the cold electron temperature to hot electron temperature is sufficiently small. The theory also predicts that the cold electrons will be preferentially heated in the perpendicular direction [Ashour-Abdalla and Kennel, 1978b]. These predictions are supported by observations by Wrenn et al. [1979] which show a good correlation between $3f_g^-/2$ emissions and highly anisotropic distributions of a few tens of eV electrons. Hence, it is possible the instability is nonlinearly saturated by heating in the cold electron distribution before the free energy in the hot distribution can be dissipated.

The above observations and discussion lead to a hypothetical, but reasonable, scenario. We suggest that intense electrostatic waves may be driven by a wide variety of distribution functions which have a source of free energy and a considerable population of cold electrons. The convective properties of the waves result in large spatial growth rates or a nonconvective instability. The waves, in turn, heat the cold electrons forming the basis of a nonlinear saturation mechanism [Ashour-Abdalla et al., 1979]. It is also possible, however, that in some cases anisotropy in the cold electron distribution may actually provide the free energy for the instability.

Acknowledgments. The research at The University of Iowa was supported by the National Aeronautics and Space Administration through Contracts NAS5-20093 and NAS5-20094, and Grant NGL-16-001-043. The research at the University of California, Los Angeles, was supported by NASA through Grant NGL-05-007-190 and NSF through Grant ATM-76-13792.

References

Ashour-Abdalla, M., and C. F. Kennel, Multi-harmonic electron cyclotron instabilities, *Geophys. Res. Lett., 5,* 711, 1978a.

Ashour-Abdalla, M., and C. F. Kennel, Nonconvective and convective electron cyclotron harmonic instabilities, *J. Geophys. Res., 83,* 1531, 1978b.

Ashour-Abdalla, M., C. F. Kennel and D. D. Sentman, Magnetospheric multi-harmonic instabilities, in *Astrophysics and Space Science Book Series,* ed. by P. J. Palmadesso, D. Reidel, Dordrecht, Netherlands, 1979.

Christiansen, P. J., M. P. Gough, G. Martelli, J. J. Block, N. Cornilleau, J. Etcheto, R. Gendrin, C. Beghin, P. Decreau, and D. Jones, GEOS-1 observations of electrostatic waves, and their relationship with plasma parameters, *Space Sci. Rev., 22,* 383, 1978.

Frank, L. A., D. M. Yeager, H. D. Owens, K. L. Ackerson and M. R. English, Quadrispherical Lepedeas for ISEE's-1 and -2 plasma measurements, *Geoscience Electronics, GE-16,* 221, 1978.

Gurnett, D. A., F. L. Scarf, R. W. Fredricks and E. J. Smith, The ISEE-1 and ISEE-2 plasma wave investigation, *Geoscience Electronics, GE-16,* 225, 1978.

Hubbard, R. F., and T. J. Birmingham, Electrostatic emissions between electron gyroharmonics in the outer magnetosphere, *J. Geophys. Res., 83,* 4837, 1978.

Kurth, W. S., J. D. Craven, L. A. Frank and D. A. Gurnett, Intense electrostatic waves near the upper hybrid resonance frequency, *J. Geophys. Res., 84,* 4145, 1979a.

Kurth, W. S., M. Ashour-Abdalla, L. A. Frank, C. F. Kennel, D. A. Gurnett, D. D. Sentman and B. G. Burek, A comparison of intense electrostatic waves near f_{UHR} with linear instability theory, *Geophys. Res. Lett., 6,* 487, 1979b.

Rönnmark, K., H. Borg, P. J. Christiansen, M. P. Gough and D. Jones, Banded electron cyclotron harmonic instability—a first comparison of theory and experiment, *Space Sci. Rev., 22,* 401, 1978.

Sentman, D. D., L. A. Frank, C. F. Kennel, D. A. Gurnett and W. S. Kurth, Electron distribution functions associated with electrostatic emissions in the dayside magnetosphere, *Geophys. Res. Lett., 6,* 781, 1979.

Wrenn, G. L., J. F. E. Johnson and J. J. Sojka, Stable 'pancake' distributions of low energy electrons in the plasma trough, *Nature, 279,* 512, 1979.

(Received October 31, 1979;
revised February 5, 1980;
accepted February 25, 1980.)